Elsevier Editorial System(tm) for Chemical Engineering Science
Manuscript Draft

Manuscript Number:

Title: From the design to the development of a continuous fixed bed photoreactor for photocatalytic degradation of organic pollutants in wastewater

Article Type: Regular Article

Section/Category: Reaction Engineering and Catalysis

Keywords: Fixed bed continuous photoreactor; design and development; visible light; UV light; wastewater treatment.

Corresponding Author: Dr. Vincenzo Vaiano,

Corresponding Author's Institution: University of Salerno

First Author: Vincenzo Vaiano

Order of Authors: Vincenzo Vaiano; Olga Sacco; Domenico Pisano; Diana Sannino; Paolo Ciambelli

Abstract: For industrial applications of photocatalytic processes aimed to the removal of pollutants from wastewater, a good solution for a final scale-up would be the choice of a continuous catalytic fixed bed photoreactor, able to work both with artificial light and with solar light. The optimal design needs a deep study starting from fluid dynamic considerations, together with the evaluation of the light's distribution inside the reactor core. In this work, flat plate geometry was chosen and a structured bed photoreactor for wastewater treatment was designed and implemented starting from an optimized N-doped TiO2 photocatalyst immobilized on glass spheres. The fluid dynamic study of the structured bed reactor was intensely carried out through a CFD model. Instead of the traditional LVRPA, the Helmholtz equation, set with the Dirichlet conditions on the boundary, was used to model the light distribution inside the photoreactor. Based on the results of the modelling optimization, a laboratory scale photoreactor was developed. In order to obtain kinetic parameters, photocatalytic tests were carried out using a model pollutant. The Langmuir-Hinshelwood kinetic model was applied for estimating the kinetic parameters of the catalyst, starting from experimental data collected at different inlet pollutant concentration. The kinetic expression together with the photons' spatial distribution was incorporated in the mass balance to achieve the theoretical distribution of the pollutant concentration in the reactor. The model was validated comparing the experimental data obtained at different contact times. The developed mathematical modeling allows to determine the best operating conditions to optimize the irradiation and the reactor volume, being a flexible method for a further scale-up of the photoreactor. The developed flat plate structured bed photoreactor was able to operate in continuous mode.

Suggested Reviewers: Mohammad Hajaghazadeh
Department of occupational Health , Urmia University of Medical Sciences
hajaghazadeh@gmail.com

JULIE MURCIA MESA
nstituto de Ciencia de Materiales de Sevilla, Universidad de Sevilla
juliejoseane@yahoo.es

Giovanni Palmisano
Department of Chemical and Environmental Engineering, Masdar Institute of Science and Technology
gpalmisano@masdar.ac.ae

Marco Stoller
Department of Chemical Materials, Environmental Engineering, Sapienza University of Rome
marco.stoller@uniroma1.it

Gian Luca Chiarello
Dipartimento di Chimica Fisica ed Elettrochimica, University of Milano
gianluca.chiarello@unimi.it

Giuseppina Iervolino
Department of Industrial Engineering, University of Salerno
giiervolino@unisa.it

Opposed Reviewers:

Dear Editor,

I kindly ask you to consider for possible publication our research paper in "**Chemical Engineering Science**".

The title of our paper is:

From the design to the development of a continuous fixed bed photoreactor for photocatalytic degradation of organic pollutants in wastewater

The manuscript is an original and novel contribution and relevant to topics of interest for this journal. It is anticipated that the manuscript will have an impact based on our experience in the field.

For industrial applications of photocatalytic processes aimed to the removal of pollutants from wastewater, a good solution for a final scale-up would be the choice of a continuous catalytic fixed bed photoreactor, able to work both with UV light and visible light. The optimal design needs a deep study starting from fluid dynamic considerations, together with the evaluation of the light's distribution inside the core of the reactor. The result of fluid dynamic modeling together with light intensity profile was used to implement a Laboratory scale photoreactor. In order to obtain kinetic parameters using the optimized design, photocatalytic tests were carried out using a model pollutant. The experimental results showed that pollutant's conversion increased with contact time both using UV and visible light sources. The Langmuir–Hinshelwood kinetic model was applied for estimating the kinetic parameters of the structured catalyst starting from experimental data collected at different pollutant inlet concentration and this kinetic model was validated with different contact times.

Sincerely,

The corresponding author.
Vincenzo Vaiano, Ph.D.
Department of Industrial Engineering
University of Salerno,
Via Giovanni Paolo II 132, 84084 Fisciano (Sa), Italy
Phone (089) 964006
Email: vvaiano@unisa.it

***Highlights (for review)**

- Design and development of a continuous flat-plate fixed bed photoreactor
- Visible light active N-doped TiO_2 photocatalyst supported on glass spheres
- Fluid dynamic conditions were chosen to have plug flow behavior
- The photons distribution has been modeled by using the Helmholtz equation
- The kinetic behavior of the photoreactor was studied by Langmuir–Hinshelwood model

From the design to the development of a continuous fixed bed photoreactor for photocatalytic degradation of organic pollutants in wastewater

V. Vaiano*, O. Sacco, D. Pisano, D. Sannino, P. Ciambelli

University of Salerno, Department of Industrial Engineering, Via Giovanni Paolo II 132, 84084 Fisciano (SA), Italy

* Corresponding author: Tel: + 39 089 964006; Fax: + 39 089 964057; E-mail: vvaiano@unisa.it.

Abstract

For industrial applications of photocatalytic processes aimed to the removal of pollutants from wastewater, a good solution for a final scale-up would be the choice of a continuous catalytic fixed bed photoreactor, able to work both with artificial light and with solar light. The optimal design needs a deep study starting from fluid dynamic considerations, together with the evaluation of the light's distribution inside the reactor core. In this work, flat plate geometry was chosen and a structured bed photoreactor for wastewater treatment was designed and implemented starting from an optimized N-doped TiO_2 photocatalyst immobilized on glass spheres. The fluid dynamic study of the structured bed reactor was intensely carried out through a CFD model. Instead of the traditional LVRPA, the Helmholtz equation, set with the Dirichlet conditions on the boundary, was used to model the light distribution inside the photoreactor. Based on the results of the modelling optimization, a laboratory scale photoreactor was developed. In order to obtain kinetic parameters, photocatalytic tests were carried out using a model pollutant. The Langmuir–Hinshelwood kinetic model was applied for estimating the kinetic parameters of the catalyst, starting from experimental data collected at different inlet pollutant concentration. The kinetic expression together with the photons' spatial distribution was incorporated in the mass balance to achieve the theoretical distribution of the pollutant concentration in the reactor. The model was validated comparing the experimental data obtained at different contact times. The developed mathematical modeling allows to determine the best operating conditions to optimize the irradiation and the reactor volume, being a flexible method for a further scale-up of the photoreactor. The developed flat plate structured bed photoreactor was able to operate in continuous mode.

Keywords: Fixed bed continuous photoreactor, design and development, visible light; UV light; wastewater treatment.

1. Introduction

During the past 30 years, the advanced oxidation processes (AOPs) have been increased considerably for involving the use of light irradiation and catalysts for treating gaseous streams and wastewater containing refractory and inhibitory organics (Palmisano et al., 2009; Parrino et al., 2014; Sannino et al., 2013a; Sannino et al., 2013b; Sannino et al., 2013c).

Titanium dioxide (TiO_2) photocatalyst in the anatase form seems to have the most interesting attributes, such as high stability, good performance and low cost (Fujishima and Zhang, 2006; Ruzmanova et al., 2013; Stoller et al., 2011). In this respect, the photodecomposition ability of TiO_2 can be advantageously used to mineralize a wide variety of pollutants present in water (Ahmed et al., 2011; Sacco et al., 2015; Vaiano et al., 2015).

The most useful reactors for the wastewater treatment are heterogeneous phototoreactors, where the photocatalysts can be present in suspended modes (slurry reactor) or immobilized on transparent support (fixed bed reactor). Most of the early photoreactors have employed a TiO_2 suspension because it offers a high surface area for the reactions. The disadvantages of the slurry photocatalysis include 1) difficulty and time consuming process of separation or filtration of the photocatalyst after the photocatalytic process; 2) particle aggregation and agglomeration at high photocatalyst concentration; and 3) difficulty of using the suspended photocatalyst in continuous processes (Sopyan et al., 1996). To overcome these drawbacks, immobilized photocatalysts are usually recommended. Photocatalysts could be immobilized on various supports such as glasses (Neti et al., 2010; Wang et al., 2014), silica (Van Grieken et al., 2002), polymers (Kasanen et al., 2009; Vaiano et al., 2014), and clays (An et al., 2008).

The efficiency of an immobilized system is less than the slurry photoreactor's one, but the photocatalyst is continuously used for a longer period of time.

In spite of the potential advantages of using photocatalytic reactors, there are still issues to be addressed. One of the main problems in photocatalytic reaction engineering is correspondent to the photoreactor scale-up.

Different literature approaches were used for modeling a large scale photoreactor.

The scale-up can be facilitated by the availability of simpler mathematical models that retain the essential elements of rigorous models but are easier to use for scale-up and design purposes (Ghafoori et al., 2014).

One of the most robust methods to design a large-scale photoreactor is to use a precise simple mathematical modeling that involves at least four sub-models that are cross-linked to the material and energy balances. These sub-models are as follows: (1) a radiation emission model (Alfano and Cassano, 2009; Marugán et al., 2009), (2) a radiation absorption-scattering model, (3) a fluid-dynamic model, and (4) a kinetic model.

The design of the photoreactor needs to start from considering the fluid flow across the photocatalytic packed bed. This has to be done to develop a system with no recirculation or dead zones. In order to achieve this design, different solutions could be taken into account, with a final goal of obtaining a plug-flow behavior inside the packed bed.

However, it is necessary to take into account that the performances of a photoreactor strictly depend also on the light sources and the light distribution inside the reactor volume.

Therefore, in order to carry out a practical scaling-up and to optimize a photoreactor, special considerations to the radiant existence must be taken into account. In fact,

precise determination of the radiation field is a difficult task. One major problem is the lack of suitable radiation models as well as kinetic models and design procedures (Li Puma and Brucato, 2007; Li Puma and Yue, 2003). Particularly, the behavior of light inside the heterogeneous media and its impact on the pollutant local degradation rate are still not well understood (Minero, 1999) .

Regarding photocatalytic reaction engineering, the Local Volumetric Rate of Photon Absorption (LVRPA) is a property of major interest (Li Puma, 2005).

It is important to mention that the LVRPA has been only indirectly estimated solving the radiative transfer equation (RTE) (Alfano et al., 2000; Brandi et al., 2000).

Moreover, the accurate determination of the LVRPA spatial distribution within the photocatalytic reactor is an important factor (Alfano et al., 1994), mainly due to both the inability to render precise kinetic information from averaged photon absorption rates (Brandi et al., 2003) and the strong non-uniformities inherent to light propagation in scattering-absorption media.

Practically, it is possible to measure the light intensity only on certain subsets of physical space (e.g. on some surfaces) surrounding the solid. Therefore, the problem arises how to reconstruct the radiation field from such experimental data (Millar, 1983).

Recently, the light distribution inside the solid media was modeled by the Helmholtz equation with two constant parameters, the scattering coefficient and the absorption coefficient (Mottin et al., 2010). This equation has been studied in various applications including biomedical imaging (Arridge, 1999), impedance imaging (Bryan and Leise, 2010) and wave propagation and scattering (Bryan and Leise, 2010). No paper reports the use of the Helmholtz equation to describe the photons' distribution in the reaction zone.

The aim of the present paper is to show a simple method for the scale-up of a continuous fixed bed photocatalytic reactor for wastewater treatment, through i) studies of fluid dynamic conditions in order to obtain a plug flow behavior inside the photocatalytic bed ii) the choice of the geometric characteristics for maximizing the exposition of the catalyst to the light sources iii) modeling of photons' distribution inside the photoreactor (Helmholtz equation).

With the designed continuous photocatalytic reactor, the influence of contact time on photocatalytic performances has been analyzed and the evaluation of kinetic parameters has been achieved using the experimental data and results obtained from the light distribution in the reactor. Finally, the developed mathematical model has been used to determine the best irradiation conditions with the aim to minimize the reactor volume.

2. Reactor design

2.1 Synthesis of structured photocatalyst (N-doped TiO_2 on glass spheres)

For the design and the final implementation of the continuous fixed bed photoreactor, firstly the visible light active N-doped TiO_2 photocatalyst was immobilized on pyrex spheres (d_p=4.3 mm, from Microglass Heim) through dip-coating technique (Vincenzo Vaiano, 2015).

Before dip-coating, the whole surface of glass spheres was rinsed with MilliQ grade water and calcined at 450°C for 30 minutes. N-doped TiO_2 coating was prepared by immersing the glass spheres support in a solution of Triton X-100 (nonionic surfactant, Sigma–Aldrich) as binder (Rosu et al., 2009). Triton X-100 was dissolved in isopropyl alcohol (i-PrOH, 99.8 wt %, Sigma–Aldrich) and the pH of solution was adjusted with nitric acid (HNO_3, 65 wt %, Carlo Erba) until to reach a value of about 2. Then, titanium (IV) isopropoxide (TTIP, 97%, Sigma–Aldrich), used as titania

precursor, was added to the mixture. The synthesis temperature of N-doped TiO_2 on glass spheres was -20°C.

Once the solution reached the temperature conditions, an ammonia aqueous solution (30 wt %, Sigma–Aldrich) was added as nitrogen precursor. The molar ratio N/Ti was equal to 18.6 and corresponds to an optimized catalyst formulation found in a previous work (Sacco et al., 2012). The glass spheres were maintained in the solution for 10 minutes and then calcined for 30 minutes at 450°C. The dip-coating procedure was repeated four times until to reach the amount of N-doped TiO_2, equal to 0.34wt%, and corresponding to the optimal loading.

2.2. Design of the fixed bed reactor: choice of the photoreactor geometry

The geometry of a photoreactor is strongly related to the source of irradiation, in particular, it has to be designed so as to collect the maximum of emitted light and to reduce the energy and investment costs. Packed bed reactors have usually an annular geometry and it is irradiated by a central lamp (Al-Ekabi et al., 1989). One of the main limits of this configuration is the uneven or partial photocatalyst's irradiation. Moreover, the uneven flow distribution also limits the amount of water in contact with the photocatalyst, negatively influencing the overall photoreactor performances (Moreira et al., 2010; Salaices et al., 2001, 2002; Serrano et al., 2010). With respect to the annular photoreactors, a flat plate geometry is scalable, and these types of reactors can be easily used with solar radiation, so they are very attractive and also provide an excellent configuration for efficient excitation of the visible light active photocatalysts (Otálvaro-Marín et al., 2014). The flat plate reactor design possesses: i) a fluid flow free from any dead or recirculation zones, obtaining a plug flow reactor; ii) ability to operate under a wide range of liquid flow rates (flow regime should also be chosen carefully in order to avoid excessive velocities, turbulences

and shear stresses that might damage the surface of the catalysts); iii) ability to be easily and efficiently integrated with an illumination system, in order to obtain the maximum model simplicity (the design of the reactor and the illumination system is aimed to deliver a high uniformity of the radiation field on the photocatalytic surface); iv) possibility to be configured for both liquid and structured catalyst side illumination (Vezzoli et al., 2013).

2.3. Design of the fixed bed reactor: fluid dynamic conditions

The preliminary special domain used for the fluid dynamic modeling of the flat plate reactor system is depicted in Figure 1; because of the axial symmetry of the problem, it was studied on a semi-transversal section of the real domain. In the investigated flat plate reactor, a water flow is pumped through a 1 cm ID tube and it is send to the body of the reactor, filled by a packed bed of the structured photocatalyst. A bar is positioned over the inner zone to avoid the plug of the inlet by the structured photocatalyst. The photoreactor operates in continuous mode at steady-state condition. The modeling of the system was performed by using the software COMSOL Multiphysics 5.0 (License No.13073437,00-0f-fe-0a-73-34). The numerical simulation has been performed by COMSOL applying the finite elements method. The final mesh, after an independent study based on the knowledge of the physics indicated below, was constituted by 150849 volume elements, 16161 surface elements and 951 elements on edges. The fluid dynamics simulation was performed by assuming incompressible and isothermal flow (the temperature was set up to 293.15 K), by using the following physics:

- Free and porous media flow: modeling of the structured photocatalyst packed bed, together with the photoreactor zones free from filling components, from

the point of view of a thermo-fluid problem, from which the fluid velocity components and pressure can be calculated;

In order to determine the velocity profiles for the laminar flow (Re < 15 for the system under investigation), inside the zones free from filling components, steady-state incompressible Navier–Stokes equations (Eq.1-2) are used for the momentum balance. So, the governing equations for continuity and the momentum balances could be written as follows:

$$\nabla \cdot u = 0 \qquad \text{Eq.1}$$

$$\rho(v \cdot \nabla)v = \nabla \cdot [-pI + \mu(\nabla v + (\nabla v)^T)] \qquad \text{Eq.2}$$

Where:

ρ = *fluid density, kg* m^{-3}

v = *velocity vector, m* s^{-1}

p = *pressure, Pa*

I = *identity matrix*

μ = *fluid dynamic viscosity, Pa s*

The boundary conditions are as follows: in the inlet section the volumetric flow rate was fixed (2.5 L h^{-1}); on the contrary, at the outlet section atmospheric pressure was fixed. Moreover, no slip boundary condition was considered for all walls of the photoreactor and the structured photocatalyst. The porous medium (that is the structured photocatalyst packed bed) was modeled using the Brinkman equation (Eq.3), which can be written as follows:

$$\frac{\rho}{\varepsilon_p}\left((v \cdot \nabla)\frac{v}{\varepsilon_p}\right) = \nabla \cdot \left[-pI + \frac{\mu}{\varepsilon_p}(\nabla v + (\nabla v)^T) - \frac{2\mu}{3\varepsilon_p}(\nabla \cdot v)I\right] - \frac{\mu}{k}v \qquad \text{Eq.3}$$

Where:

ε_p = *bed porosity = 0.55*

k = bed permeability, m^2

The latter can be calculated easily by the Rump-Gupte equation (Eq.4) (Fatehi and Kaviany, 1994):

$$k = \frac{\varepsilon_p^{5.5}}{5.6} d^2 \qquad \text{Eq.4}$$

Where:

d = glass spheres diameter = 4.3 mm

In order to determine how the thickness of the reactor influences the velocity profiles inside the flat plate reactor, thickness was varied in the range (1<y<4 cm). The results of the mathematical modeling are shown in Figure 2. In particular, Figure 2 shows the behavior at a specific reactor thickness (2.5 cm) along the reactor height in terms of average velocity-maximum velocity ratio ($\bar{v}/v_{\max}$), which could be related to the length of entrance, or the length at which the velocity profile is fully developed. The results demonstrated that over the inlet tube (z=1 cm) there is a zone in which the profile is continuously developing. Actually, at the bed inlet, the $\bar{v}/v_{\max}$ ratio is very close to its maximum value, which is sign of fully developed profile. In particular, inside the bed, the average velocity value is very close to the v_{max}, so the profile ought to be almost flat. The same behavior, in terms of $\bar{v}/v_{\max}$ profile along the reactor height, could be observed by varying the reactor thickness, in all cases. The velocity profile with a thickness of 2.5 cm, is fully developed at a reactor height lower than that one observed for reactor thickness higher or lower than

2.5 cm. Besides, the inset of Figure 2 shows that the trend of $\bar{v}/v_{max}$ ratio at the bed inlet against the reactor thickness (y-direction) has a maximum value at 2.5 cm. This means that, at this specific thickness, the approach to the fully developed profile inside the photocatalytic bed is faster, i.e. definitely the whole packed bed zone shows a plug flow behavior. Moreover, in Figure 3a it is possible to observe the flow lines along the photoreactor, while in Figure 3b the flat profile which is developed inside the packed bed. So, this simulation demonstrates that this type of reactor configuration allows to obtain a plug flow behavior inside the photocatalytic bed, which guarantees a perfect homogenization of the fluid across the reactor width.

2.4. Design of the fixed bed reactor: radiative transfer model

The photons' distribution inside the photoreactor has been modeled by using the Helmholtz equation:

$$\nabla \cdot \left(-c\nabla I\right) + aI = f \qquad \text{Eq.5}$$

Where :

$c = \dfrac{1}{3(d+a)}$ = *diffusion coefficient, cm*

I= light intensity,W cm^{-2}

a= structured catalysts absorption coefficient, cm^{-1}

d= structured catalysts scattering coefficient, cm^{-1}

f= source term=0

The source term *f* in this case is equal to zero because no light source is present inside the reactor.

The values of *a* and *d* have been estimated from UV-vis DRS spectra of the N-doped TiO_2 photocatalyst supported on glass spheres following the method reported in

(Vincenzo Vaiano, 2014), that strictly depends on the emission spectrum of the light source. With this method, *a* and *d* were found equal to 78 and 22 cm^{-1}, respectively.

In order to simplify technical details of the analysis, the boundary Dirichlet condition was chosen on the external windows of the reactor. In a preliminary configuration, an 8 Watt UV-lamp provided by Philips was used. The UV-lamp has a cylindrical shape with a diameter of 1.6 cm and a height of 27 cm. This lamp has an emission spectrum centered at 365 nm (Vincenzo Vaiano, 2014). The UV-light intensity at the external surface of the lamps was measured by a UV meter and it is equal to 0.023W cm^{-2}.

The lamps in this case cover the entire transparent surfaces of the reactor. So, the preliminary height of the reactor was chosen equal to the height of the UV lamps. For what regards the photoreactor thickness, taking into account the results obtained by the fluid dynamic evaluation, it was chosen equal to 2.5 cm.

The numerical simulation has been performed by COMSOL applying the finite elements method. The final mesh, after an independent study based on the knowledge of the specific physics, was constituted by 9834 volume elements, 9834 surface elements and 1330 elements on edges.

The results of the mathematical solution of Helmholtz equation are reported in Figure 4.

The simulation of the light distribution shows that the light profile, by using the 8 Watt UV-lamps, is characterized by a strong attenuation of the light intensity (almost 70%) inside the core of the reactor.

2.5. Design of the fixed bed reactor: final design

Among the types of photoreactor design, the flat plate reactor seems to be the more flexible choice for the scale-up, because it is the best compromise between

construction and irradiation features. In order to optimize the design of the photoreactor, it is needed to take into account the results obtained by the fluid dynamics and the photons' distribution simulation along the reactor width. In particular, in this case the only design variable was the reactor thickness, because it is the only one that can affect significantly both the fluid dynamic behavior and the photons' distribution. So, for the final design, it was considered a reactor thickness equal to 2.5 cm, because it guarantees a plug flow behavior inside the structured bed and at the same time minimizes the photons' loss inside the core of the rector.

3. Photocalytic activity tests with the designed continuous fixed bed reactor

3.1 Laboratory scale photoreactor

The schematic diagram of the laboratory scale photoreactor is shown in Figure 5.

The laboratory scale photoreactor geometry designed as shown in the previous sections is composed by a flat plate body with two pyrex windows irradiated by five UV (provided by Philips; nominal power: 8 Watt) or visible light (provided by Philips; nominal power: 8 Watt) sources for each window respectively (Figure 5). The photoreactor operates in continuous mode at steady-state condition. The stock solution containing the pollutant to be removed was prepared and collected in the feed tank. The feed tank is equipped with a propeller to assure the complete homogenization of the stock solution, and an air distributor device (Q_{air}=150cm^3 min^{-1} (STP)).

The feed solution was pumped from the feed tank to the photoreactor using two peristaltic pumps (Watson Marlowe 120s) capable of producing a liquid flow rate in the range 0.56-2.5L h^{-1}. The overall liquid stream is fed from the bottom of the reactor by means of two stainless steel tubes with ID equal to 1 cm. The amount of structured catalyst was equal to 372 g. The liquid stream passes through the

310 photocatalytic bed and finally comes out from the top of the reactor, being collected
311 in a tank. The liquid sample was withdrawn on the top of the photocatalytic bed.

312 The pH of the reaction mixture was not adjusted (natural solution pH) and the
313 temperature was controlled before and after the flat plate body, in particular it varies
314 from 20 to 30°C. In order to obtain the kinetic parameters using the optimized
315 design, photocatalytic tests were carried out using methylene blue (MB) as model
316 pollutant.

317 Liquid samples were analyzed by spectrophotometric measurements (Perkin Elmer
318 UV-Vis spectrophotometer at $\lambda = 663$ nm) in order to determine the changes in MB
319 concentration.

320 *3.2 Experimental results using UV or visible light sources*

321 The photocatalytic tests were carried out using MB inlet concentration equal to 10
322 ppm.

323 The light sources were switched on after the complete adsorption of MB on the
324 structured catalysts surface. Preliminary experiments were carried out in order to
325 verify that MB was degraded by the heterogeneous photocatalytic process. In the
326 absence of structured catalyst, no significant decrease in MB concentration was
327 observed during illumination, both with UV light and visible light irradiation.

328 The MB conversion profiles, as function of contact time at steady-state conditions
329 obtained in presence of UV and visible light irradiation, are reported in Figure 6. It
330 can be seen that MB conversion increased with the increase of the contact time when
331 UV light was applied, in the presence of the structured photocatalyst, in fact, MB
332 conversion reached a value of about 75% for a contact time equal to 2.5 h.

It was also performed visible light driven photocatalytic degradation of MB over the structured catalyst and the results are presented in Figure 6. It was observed, also in this case, that the presence of the structured catalyst led to a significant removal rate, with a MB conversion equal to 50% for a contact time equal to 2.5 h. This is a very interesting result, in view of the implementation of a photoreactor, which would be processed also with a solar light irradiation.

3.3 Kinetic modeling of the continuous fixed bed reactor irradiated by UV light

From the results of Helmholtz equation obtained from COMSOL Multiphysics (version 5.0), it is clear that there is a non-homogeneous distribution of photons along the reactor thickness. To approach to the kinetic model, it could be considered the average light intensity $\bar{I}$, that can be estimated according to the Eq.6

$$\bar{I} = \frac{2 \cdot \int_0^{\frac{L}{2}} I(y) \cdot dy}{L} \qquad \text{Eq.6}$$

Where:

I(y)=light intensity profile as a function of photoreactor thickness,W.dm^{-2}

L= photoreactor thickness, cm

The kinetic model can be therefore developed considering plug flow behaviour inside the packed bed, as shown previously by the fluid dynamic study. Therefore, the MB mass balance can be written as:

$$Q\frac{dC}{dV} = r(C,\bar{I}) \cdot \rho_{cat} \qquad \text{Eq.7}$$

Where:

Q=Total liquid flow rate, L h^{-1}

354 *C=MB concentration, ppm*

355 *V= reactor volume, L*

356 ρ_{cat}*=bulk density of structured catalyst, g* L^{-1}

357 $\bar{I}$ *= average light intensity inside the photoreactor, W* dm^{-2}

358 The boundary condition for the Eq.7 is:

359 *V=0* *C=*C_0*=MB inlet concentration*

360 The kinetics of MB removal could be expressed by Eq. 8:

361 $$-r = K \cdot f_C \cdot g_I \cdot h_{C_0}$$ Eq.8

362 Where:

363 $$f_C = \frac{b \cdot C}{1 + b \cdot C}$$ Eq.9

364 $$g_I = \bar{I}$$ Eq.10

365 $$h_{C_0} = e^{-\alpha\left(\frac{b \cdot C_0}{1 + b \cdot C_0}\right)}$$ Eq.11

366 with:

367 *K=kinetic constant,* $mg_{MB}\ g_{cat}^{-1}\ h^{-1}\ W^{-1}\ dm^2$

368 *b= adsorption constant of MB,* $l\ mg^{-1}$

369 Looking at Eq. 8, Eq. 9 agrees a pseudo Langmuir-Hinshelwood rate law used in
370 other studies (Sannino et al., 2013d; Sivalingam et al., 2003).

371 The Eq.11 allows to take into account that the light penetration inside the reactor
372 decreases because of the strong blue colour assumed by the structured catalyst after
373 MB adsorption. This coloration is a function of the amount of MB adsorbed on its

surface. So, this phenomenon acts as a screening effect for the penetration of light, similarly to that one due to the increase of the catalyst concentration in a slurry photoreactor configuration (Konstantinou and Albanis, 2004; Sannino et al., 2013d).

This effect can be evaluated utilizing a screening parameter that is a function of the structured catalyst color, $\alpha(C_0)$, similar to a molar extinction coefficient in a pseudo-Lambert Beer law. The dependence from the color assumed by the structured catalyst from the initial concentration of MB is expressed trough the Langmuir-adsorption law (Eq. 9 evaluated at C_0).

3.3.1 Evaluation of adsorption constant of MB on structured photocatalyst

The adsorption equilibrium was evaluated in batch conditions monitoring the concentration of MB as function of run time for different MB concentrations. The behavior of the amount of MB adsorbed on the structured catalyst (C^*) is a function of the initial MB concentration (C_0) and it is similar to a Langmuir adsorption isotherm (Sannino et al., 2013d).

Thus, for the adsorption of MB on the active surface of the structured photocatalyst (Herney-Ramirez et al., 2010), it is possible to write:

$$C^* = \frac{b \cdot C_0}{1 + b \cdot C_0} \qquad \text{Eq.12}$$

Where:

C^*: amount of MB adsorbed [g_{MB}/g_{cat}]

*C_m: maximum absorbable value of C**

C_0:initial concentration of MB in solution [mg L^{-1}]

The Langmuir isotherm can be rearranged to give:

$$\frac{C_0}{C^*} = \frac{1}{bC_m} + \frac{1}{C_m} \cdot C_0 \qquad \text{Eq.13}$$

Plotting C_0/C^* as a function of C_0 produces a straight line with: slope=$1/C_m$ and intercept=$1/bC_m$ (Figure 7).

The value of *b* was calculated from the Eq.13, utilizing the experimental data, and it was equal to 0.01 [L mg^{-1}].

3.3.2 Evaluation of kinetic parameters

Utilizing the Eq.6 and Eq.7, MB mass balance can be written as:

$$Q \cdot \frac{dC}{dV} = -K \cdot \frac{b \cdot C}{1 + b \cdot C} \cdot \bar{I} \cdot e^{-\alpha\left(\frac{b \cdot C_0}{1 + b \cdot C_0}\right)} \rho_{cat} \qquad \text{Eq.14}$$

The Eq.14, together with the boundary condition, was solved by the Euler iterative method. From the simulation made by the mathematical model, it is possible to estimate the constants *K* and α by fitting the experimental data reported in Figure 8 as a function of inlet MB concentration in the range 3.6-16 ppm and with a liquid flow rate of 1.45 L h^{-1}. The fitting procedure was done by using the least squares approach obtaining the value of *K*: 1477 (mg_{MB} g_{cat}^{-1} $h^{-1}W^{-1}$ dm^2) and α: 43 (-).

After obtaining the kinetic parameters (*K* and α), the accuracy of the developed model was tested by comparing the calculated MB conversion with the experimental tests as function of contact time (Figure 9). The calculated values are in good agreement with the experimental data.

3.3.3 Influences of light distribution on photocatalytic performances

Since the light intensity strongly depends on the distance from the external irradiated windows, the simulated profile of MB conversion inside the reactor has been obtained according to the Eq.15

$$v_z(y)\cdot\frac{dC(z,y)}{dz}=-K\cdot\frac{b\cdot C(z,y)}{1+b\cdot C(z,y)}\cdot I(y)\cdot e^{-\alpha\left(\frac{b\cdot C_0}{1+b\cdot C_0}\right)}\rho_{cat} \qquad \text{Eq.15}$$

Where:

$v_z(y)$= *component of velocity vector along z-direction, dm* h^{-1}

In this case $v_z(y)=v_{max}$, since, as evidenced in section 2.3, the fluid dynamic conditions in the packed bed are similar to those of a plug flow, so v_{max} is the maximum velocity that is equal at any given x-direction.

Since the light intensity depends on the y-direction, at any given y the MB concentration it is only a function of the z-direction. The obtained results are reported in Figure 10. From the results it is evident that reaction rate is affected by the local photons' "concentration" since the experimental data lie in the simulated profiles.

4. Conclusions

A continuous fixed bed photoreactor for wastewater treatment was firstly designed and finally implemented. As catalyst it was used a N-doped TiO_2 immobilized on glass spheres with an optimized formulation.

Among the many different configurations of the reactor design, the flat plate geometry has been chosen to maximize the exposition of catalyst to the light sources. The fluid dynamic study in a flat plate fixed bed reactor was carried out using a CFD model (COMSOL Multiphysics 5.0) obtaining that the best reactor thickness to have plug flow conditions inside the photocatalytic bed is 2.5 cm. The model of light distribution inside the reactor was developed using the Helmholtz equation, set with the Dirichlet conditions on the boundary, evidencing that the use of UV-lamps determined a strong attenuation of light intensity (almost 70%) inside the core of the

441 reactor. The result of fluid dynamic together with light intensity profile was used to
442 implement a laboratory scale photoreactor. The experimental results obtained on the
443 developed photoreactor showed that methylene blue (used as model pollutant)
444 conversion increased with contact time both using UV and visible light sources.
445 A pseudo Langmuir–Hinshelwood kinetic model was applied for studying the kinetic
446 behaviour of the structured catalyst starting from experimental data collected at
447 different MB inlet concentration. The value of MB adsorption constant has been
448 evaluated from experimental data carried out in dark conditions.
449 The kinetic expression together with the average light intensity in the thickness of
450 reactor and the attenuation of light due to the strong blue colour induced by
451 adsorption of MB on catalyst, were incorporated in the mass balance to estimate the
452 kinetic parameters. The model has been successfully validated by comparing the
453 calculated MB conversion with the experimental tests as function of contact time.
454 Main issues were related to the photon spatial distribution inside the reactor and the
455 colouring of the catalyst, also in the optimized developed flat plate reactor
456 configuration. So, the design criteria for all type of continuous photoreactors strongly
457 depended on fluid dynamic conditions and light sources to be used, and adsorption
458 properties of the photocatalyst.
459
460

References

Ahmed, S., Rasul, M.G., Martens, W.N., Brown, R., Hashib, M.A., 2011. Advances in heterogeneous photocatalytic degradation of phenols and dyes in wastewater: A review. Water, Air, and Soil Pollution 215, 3-29.

Al-Ekabi, H., Serpone, N., Pelizzetti, E., Minero, C., Fox, M.A., Draper, R.B., 1989. Kinetic studies in heterogeneous photocatalysis. 2. TiO2-mediated degradation of 4-chlorophenol alone and in a three-component mixture of 4-chlorophenol, 2,4-dichlorophenol, and 2,4,5-trichlorophenol in air-equilibrated aqueous media. Langmuir 5, 250-255.

Alfano, O.M., Bahnemann, D., Cassano, A.E., Dillert, R., Goslich, R., 2000. Photocatalysis in water environments using artificial and solar light. Catalysis Today 58, 199-230.

Alfano, O.M., Cabrera, M.I., Cassano, A.E., 1994. Modeling of light scattering in photochemical reactors. Chemical Engineering Science 49, 5327-5346.

Alfano, O.M., Cassano, A.E., 2009. Scaling-Up of Photoreactors. Applications to Advanced Oxidation Processes, Advances in Chemical Engineering, pp. 229-287.

An, T., Chen, J., Li, G., Ding, X., Sheng, G., Fu, J., Mai, B., O'Shea, K.E., 2008. Characterization and the photocatalytic activity of TiO2 immobilized hydrophobic montmorillonite photocatalysts. Degradation of decabromodiphenyl ether (BDE 209). Catalysis Today 139, 69-76.

Arridge, S.R., 1999. Optical tomography in medical imaging. Inverse Problems 15, R41-R49.

Brandi, R.J., Alfano, O.M., Cassano, A.E., 2000. Evaluation of radiation absorption in slurry photocatalytic reactors. 2. Experimental verification of the proposed method. Environmental Science and Technology 34, 2631-2639.

Brandi, R.J., Citroni, M.A., Alfano, O.M., Cassano, A.E., 2003. Absolute quantum yields in photocatalytic slurry reactors. Chemical Engineering Science 58, 979-985.

Bryan, K., Leise, T., 2010. Impedance imaging, inverse problems and Harry Potter's cloak. SIAM Review 52, 359-377.

Fatehi, M., Kaviany, M., 1994. Adiabatic reverse combustion in a packed bed. Combustion and Flame 99, 1-17.

Fujishima, A., Zhang, X., 2006. Titanium dioxide photocatalysis: present situation and future approaches. Comptes Rendus Chimie 9, 750-760.

Ghafoori, S., Mehrvar, M., Chan, P.K., 2014. Photoreactor scale-up for degradation of aqueous poly(vinyl alcohol) using UV/H2O2 process. Chemical Engineering Journal 245, 133-142.

509 Herney-Ramirez, J., Vicente, M.A., Madeira, L.M., 2010. Heterogeneous photo-
510 Fenton oxidation with pillared clay-based catalysts for wastewater treatment: A
511 review. Applied Catalysis B-Environmental 98, 10-26.
512
513 Kasanen, J., Suvanto, M., Pakkanen, T.T., 2009. Self-cleaning, titanium dioxide
514 based, multilayer coating fabricated on polymer and glass surfaces. Journal of
515 Applied Polymer Science 111, 2597-2606.
516
517 Konstantinou, I.K., Albanis, T.A., 2004. TiO_2-assisted photocatalytic degradation of
518 azo dyes in aqueous solution: kinetic and mechanistic investigations - A review.
519 Applied Catalysis B-Environmental 49, 1-14.
520
521 Li Puma, G., 2005. Dimensionless analysis of photocatalytic reactors using
522 suspended solid photocatalysts. Chemical Engineering Research and Design 83, 820-
523 826.
524
525 Li Puma, G., Brucato, A., 2007. Dimensionless analysis of slurry photocatalytic
526 reactors using two-flux and six-flux radiation absorption-scattering models. Catalysis
527 Today 122, 78-90.
528
529 Li Puma, G., Yue, P.L., 2003. Modelling and design of thin-film slurry
530 photocatalytic reactors for water purification. Chemical Engineering Science 58,
531 2269-2281.
532
533 Marugán, J., van Grieken, R., Cassano, A.E., Alfano, O.M., 2009. Scaling-up of
534 slurry reactors for the photocatalytic oxidation of cyanide with TiO2 and silica-
535 supported TiO2 suspensions. Catalysis Today 144, 87-93.
536
537 Millar, R.F., 1983. The analytic continuation of solutions of the generalized axially
538 symmetric Helmholtz equation. Archive for Rational Mechanics and Analysis 81,
539 349-372.
540
541 Minero, C., 1999. Kinetic analysis of photoinduced reactions at the water
542 semiconductor interface. Catalysis Today 54, 205-216.
543
544 Moreira, J., Serrano, B., Ortiz, A., De Lasa, H., 2010. Evaluation of photon
545 absorption in an aqueous TiO2 slurry reactor using Monte Carlo simulations and
546 macroscopic balance. Industrial and Engineering Chemistry Research 49, 10524-
547 10534.
548
549 Mottin, S., Panasenko, G., Ganesh, S.S., 2010. Multiscale modeling of light
550 absorption in tissues: Limitations of classical homogenization approach. PLoS ONE
551 5.
552
553 Neti, N.R., Parmar, G.R., Bakardjieva, S., Subrt, J., 2010. Thick film titania on glass
554 supports for vapour phase photocatalytic degradation of toluene, acetone, and
555 ethanol. Chemical Engineering Journal 163, 219-229.
556

Otálvaro-Marín, H.L., Mueses, M.A., Machuca-Martínez, F., 2014. Boundary layer of photon absorption applied to heterogeneous photocatalytic solar flat plate reactor design. International Journal of Photoenergy 2014.

Palmisano, G., Loddo, V., Nazer, H.H.E., Yurdakal, S., Augugliaro, V., Ciriminna, R., Pagliaro, M., 2009. Graphite-supported TiO2 for 4-nitrophenol degradation in a photoelectrocatalytic reactor. Chemical Engineering Journal 155, 339-346.

Parrino, F., Camera-Roda, G., Loddo, V., Palmisano, G., Augugliaro, V., 2014. Combination of ozonation and photocatalysis for purification of aqueous effluents containing formic acid as probe pollutant and bromide ion. Water Research 50, 189-199.

Rosu, M.C., Suciu, R.C., Kasco, I., Dreve, S.V., Indrea, E., Silipas, T.D., 2009. A spectroscopic study of dyes decomposition by irradiated nanocrystalline TiO2. Journal of Physics: Conference Series 182.

Ruzmanova, Y., Ustundas, M., Stoller, M., Chianese, A., 2013. Photocatalytic treatment of olive mill wastewater by n-doped titanium dioxide nanoparticles under visible light. Chemical Engineering Transactions 32, 2233-2238.

Sacco, O., Stoller, M., Vaiano, V., Ciambelli, P., Chianese, A., Sannino, D., 2012. Photocatalytic degradation of organic dyes under visible light on n-doped TiO2 photocatalysts. International Journal of Photoenergy 2012.

Sacco, O., Vaiano, V., Han, C., Sannino, D., Dionysiou, D.D., 2015. Photocatalytic removal of atrazine using N-doped TiO2 supported on phosphors. Applied Catalysis B: Environmental 164, 462-474.

Salaices, M., Serrano, B., De Lasa, H.I., 2001. Photocatalytic conversion of organic pollutants extinction coefficients and quantum efficiencies. Industrial and Engineering Chemistry Research 40, 5455-5464.

Salaices, M., Serrano, B., De Lasa, H.I., 2002. Experimental evaluation of photon absorption in an aqueous TiO2 slurry reactor. Chemical Engineering Journal 90, 219-229.

Sannino, D., Vaiano, V., Ciambelli, P., 2013a. Innovative structured VOx/TiO2 photocatalysts supported on phosphors for the selective photocatalytic oxidation of ethanol to acetaldehyde. Catalysis Today 205, 159-167.

Sannino, D., Vaiano, V., Ciambelli, P., Carotenuto, G., Di Serio, M., Santacesaria, E., 2013b. Enhanced performances of grafted VOx on titania/silica for the selective photocatalytic oxidation of ethanol to acetaldehyde. Catalysis Today 209, 159-163.

Sannino, D., Vaiano, V., Ciambelli, P., Isupova, L.A., 2013c. Mathematical modelling of the heterogeneous photo-Fenton oxidation Of acetic acid on structured catalysts. Chemical Engineering Journal 224, 53-58.

Sannino, D., Vaiano, V., Sacco, O., Ciambelli, P., 2013d. Mathematical modelling of photocatalytic degradation of methylene blue under visible light irradiation. Journal of Environmental Chemical Engineering 1, 56-60.

Serrano, B., Ortíz, A., Moreira, J., De Lasa, H.I., 2010. Photocatalytic thermodynamic efficiency factors. Practical limits in photocatalytic reactors. Industrial and Engineering Chemistry Research 49, 6824-6833.

Sivalingam, G., Nagaveni, K., Hegde, M.S., Madras, G., 2003. Photocatalytic degradation of various dyes by combustion synthesized nano anatase TiO_2. Applied Catalysis B-Environmental 45, 23-38.

Sopyan, I., Watanabe, M., Murasawa, S., Hashimoto, K., Fujishima, A., 1996. A film-type photocatalyst incorporating highly active TiO2 powder and fluororesin binder: Photocatalytic activity and long-term stability. Journal of Electroanalytical Chemistry 415, 183-186.

Stoller, M., Movassaghi, K., Chianese, A., 2011. Photocatalytic degradation of orange II in aqueous solutions by immobilized nanostructured titanium dioxide. Chemical Engineering Transactions 24, 229-234.

Vaiano, V., Sacco, O., Sannino, D., Ciambelli, P., 2015. Photocatalytic removal of spiramycin from wastewater under visible light with N-doped TiO2 photocatalysts. Chemical Engineering Journal 261, 3-8.

Vaiano, V., Sacco, O., Sannino, D., Ciambelli, P., Longo, S., Venditto, V., Guerra, G., 2014. N-doped TiO2/s-PS aerogels for photocatalytic degradation of organic dyes in wastewater under visible light irradiation. Journal of Chemical Technology and Biotechnology 89, 1175-1181.

Van Grieken, R., Aguado, J., López-Muoz, M.J., Marugán, J., 2002. Synthesis of size-controlled silica-supported TiO2 photocatalysts. Journal of Photochemistry and Photobiology A: Chemistry 148, 315-322.

Vezzoli, M., Farrell, T., Baker, A., Psaltis, S., Martens, W.N., Bell, J.M., 2013. Optimal catalyst thickness in titanium dioxide fixed film reactors: Mathematical modelling and experimental validation. Chemical Engineering Journal 234, 57-65.

Vincenzo Vaiano, O.S., Diana Sannino, Paolo Ciambelli, 2015. Nanostructured N-doped TiO2 Coated on Glass Spheres for the Photocatalytic Removal of Organic Dyes under UV or Visible Light Irradiation. Applied Catalysis B: Environmental.

Vincenzo Vaiano, O.S., Marco Stoller, Angelo Chianese, Paolo Ciambelli, and Diana Sannino, 2014. Influence of the Photoreactor Configuration and of Different Light Sources in the Photocatalytic Treatment of Highly Polluted Wastewater. International Journal of Chemical Reactor Engineering 12, 1-13.

Wang, W., Ni, Y., Lu, C., Xu, Z., 2014. Hydrogenation temperature related inner structures and visible-light-driven photocatalysis of N-F co-doped TiO2 nanosheets. Applied Surface Science 290, 125-130.

655
656

Figure 1
Click here to download Figure: Figure 1bis .pdf

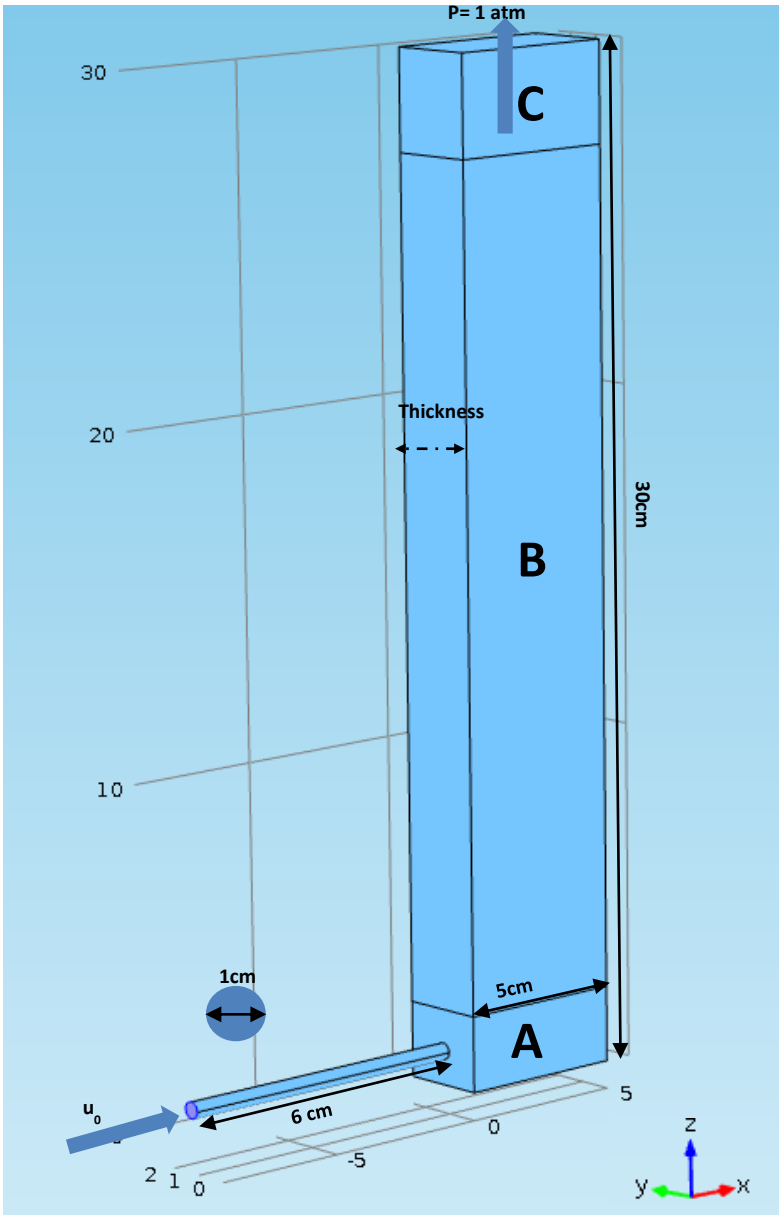

Figure 1 Preliminary domain for the fluid dynamic model where a) is the homogenization zone; b) is the body of reactor where is filled with the structured photocatalyst; c) the outlet zone

Figure 2
Click here to download Figure: Figure 2bis.pdf

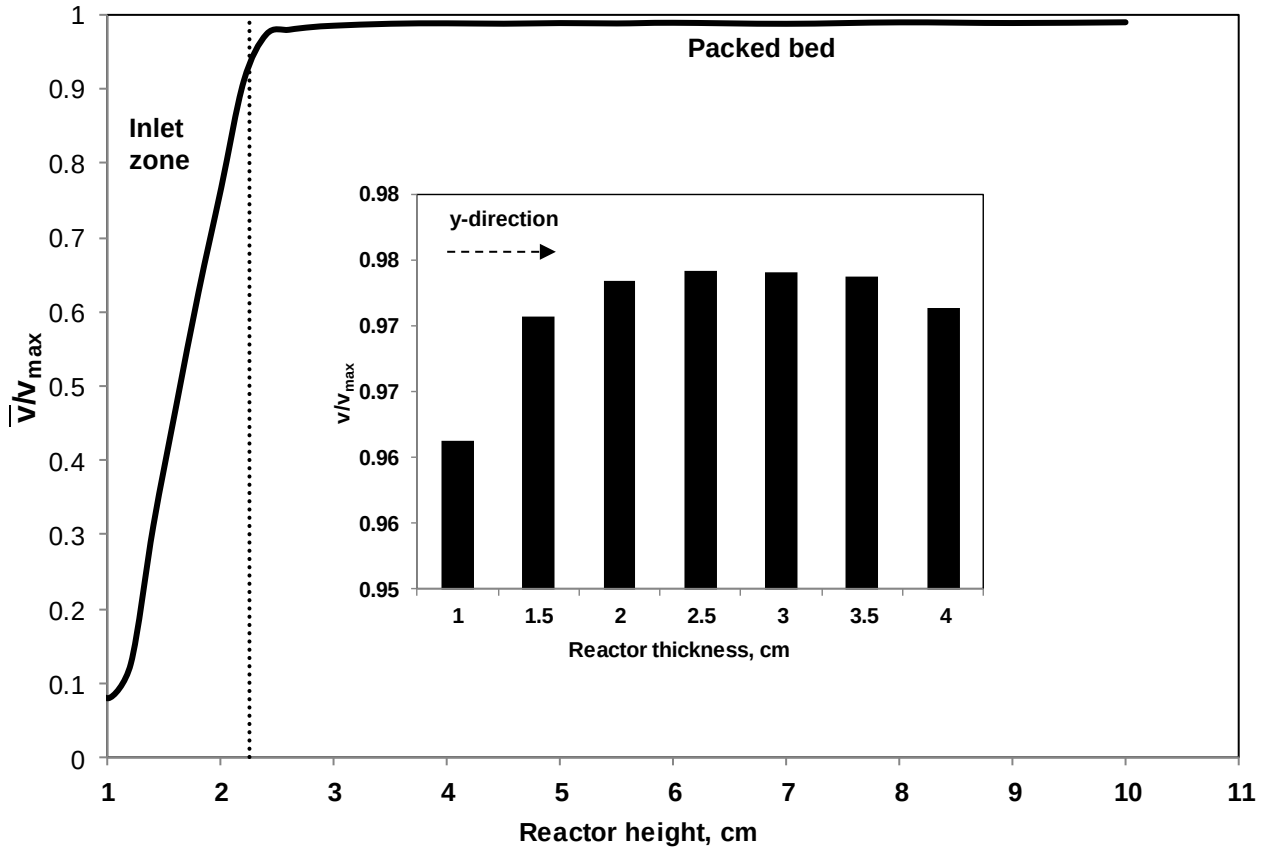

Figure 2 Behavior of $\bar{v}/v_{max}$ as a function of reactor height (z-direction) and behavior of $\bar{v}/v_{max}$ as a function of reactor thickness at the bed inlet (inset).

Figure 3
Click here to download Figure: Figure 3bis.pdf

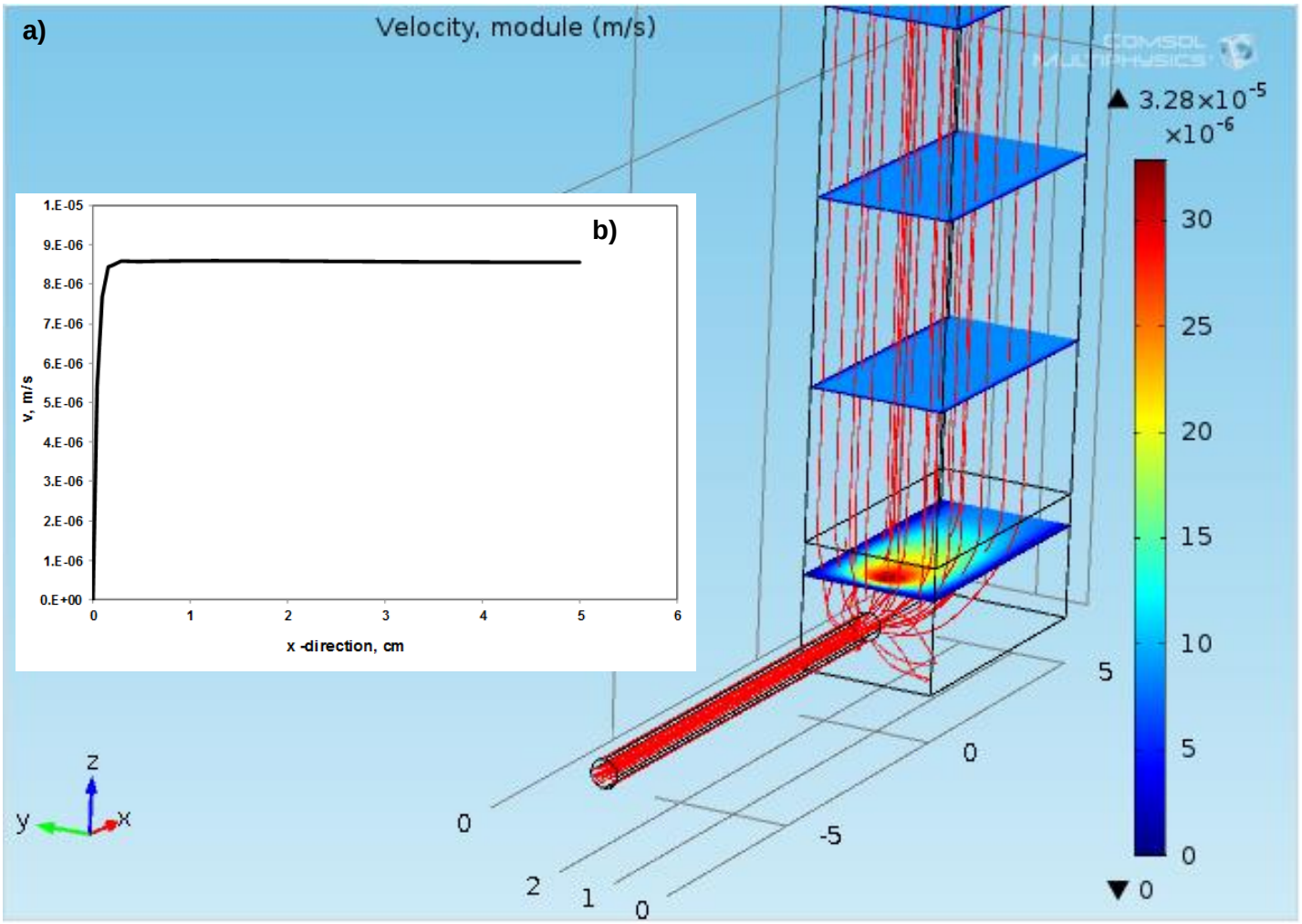

Figure 3 a) The flow lines along the photoreactor, b) Flat profile inside the packed bed

Figure 4
Click here to download Figure: Figure 4bis .pdf

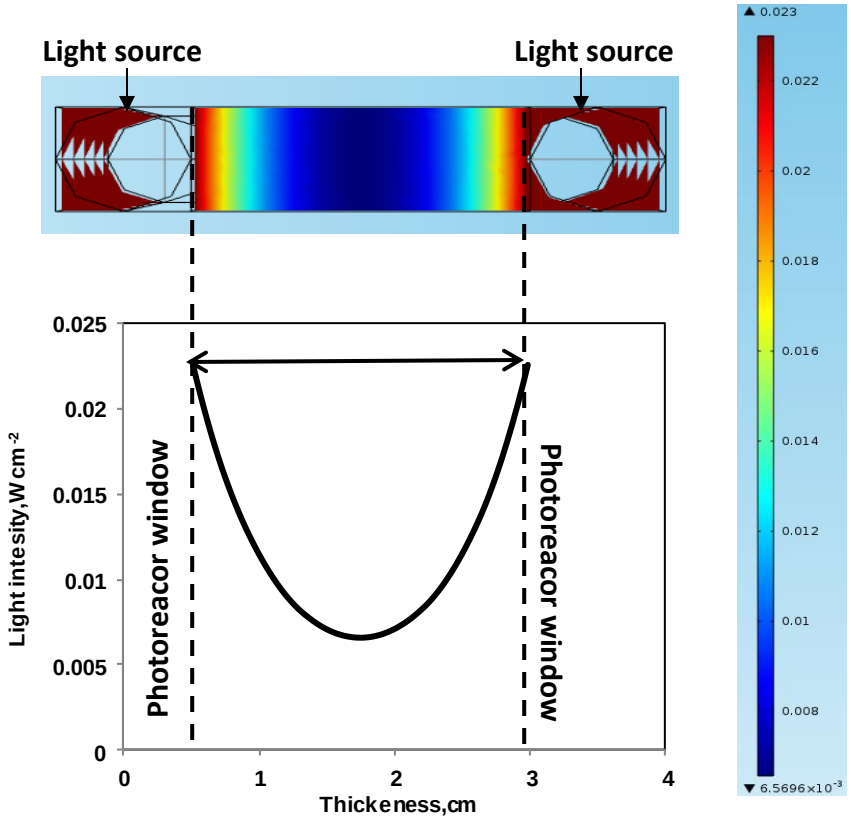

Figure 4 The Helmholtz model of light distribution inside the reactor; Light sources: UV-lamps with intensity equal to 0.023 W cm^{-2}; Reactor thickness: 2.5 cm

Figure 5
Click here to download Figure: Figure 5bis.pdf

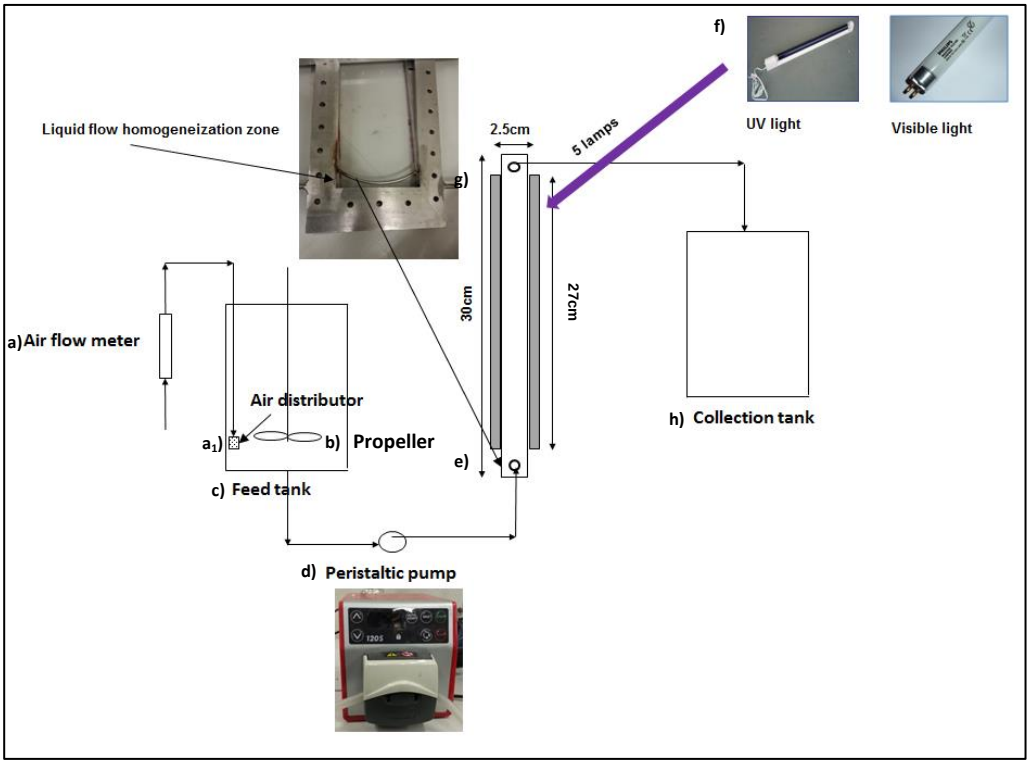

Figure 5 Experimental set up apparatus: (a) air flow meter;(a_1) air distributor; (b) propeller; (c) feed tank; (d) peristaltic pump, (e) inlet of the flow in the reactor; (f) light sources; (g) outlet of liquid flow; (h) collection tank.

Figure 6
Click here to download Figure: Figure 6.docx

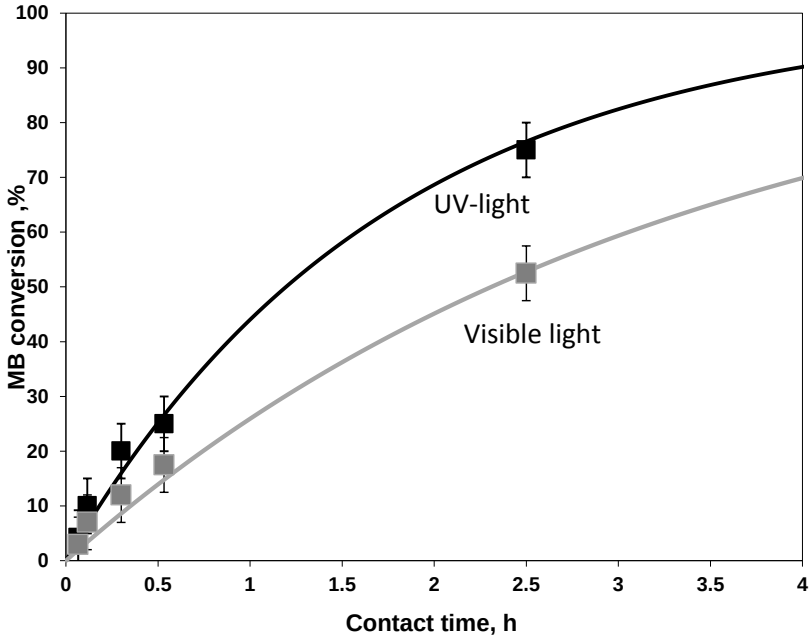

Figure 6 MB conversion profiles as function of contact time using UV or visible light irradiation

Figure 7
Click here to download Figure: Figure 7.pdf

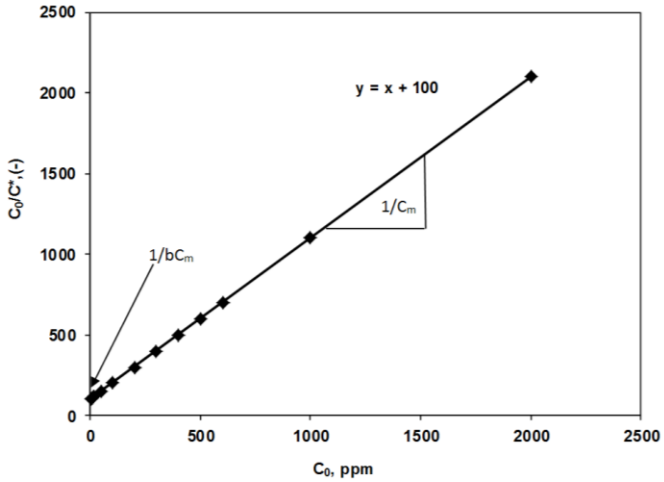

Figure 7 Evaluation of MB adsorption constant on structured catalyst

Figure 8
Click here to download Figure: Figure 8 .docx

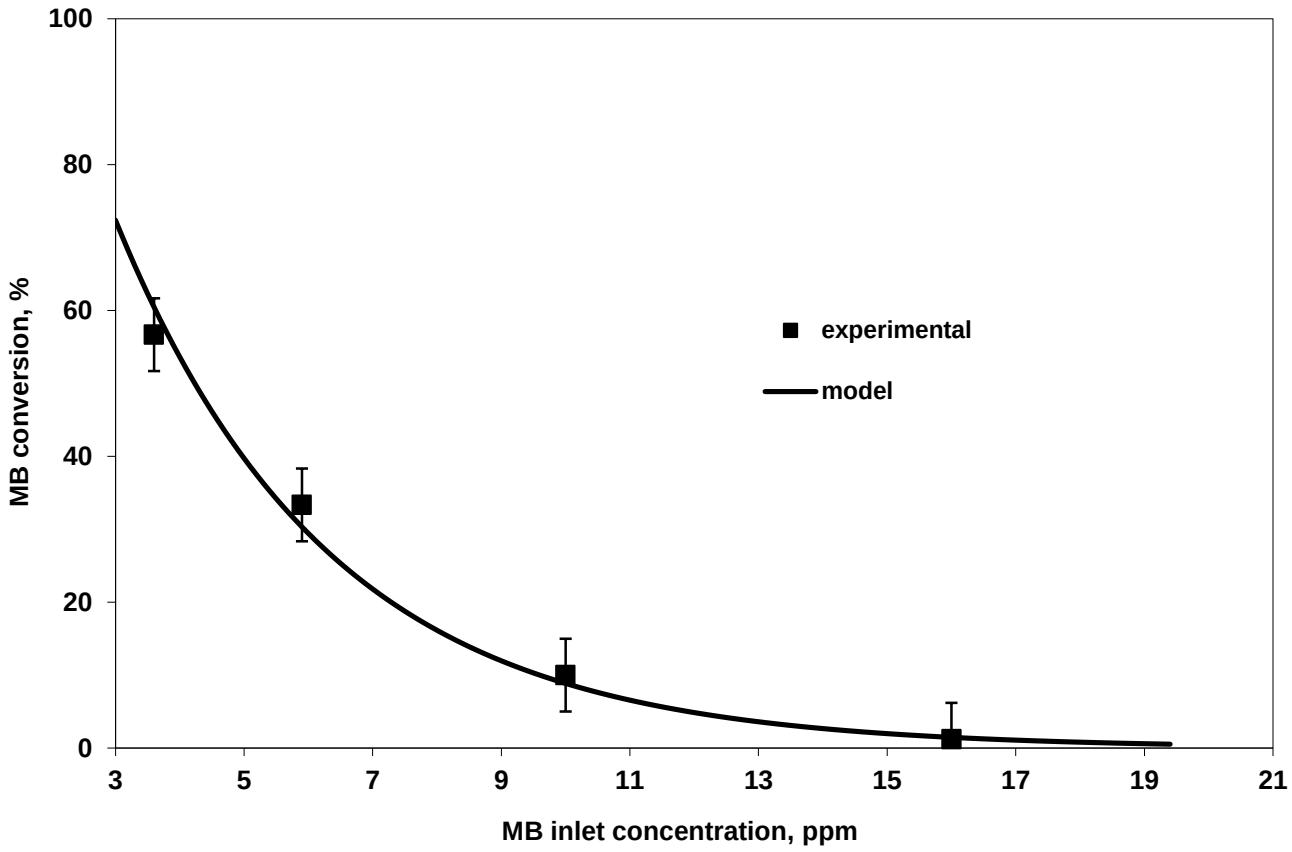

Figure 8 MB conversion as a function of inlet concentration; comparison between model calculation and experimental data to find the model constant. Light sources: UV-lamps; liquid flow rate: 1.45l h^{-1}

Figure 9
Click here to download Figure: Figure 9.pdf

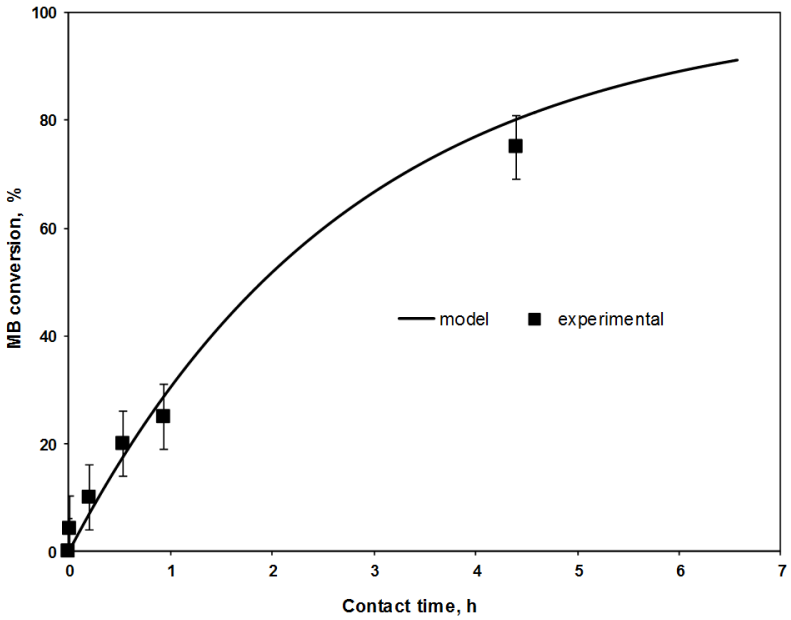

Figure 9 Experimental and predict data at different contact times Light sources: UV-lamps; inlet MB concentration. 10ppm

Figure 10
Click here to download Figure: Figure 10.docx

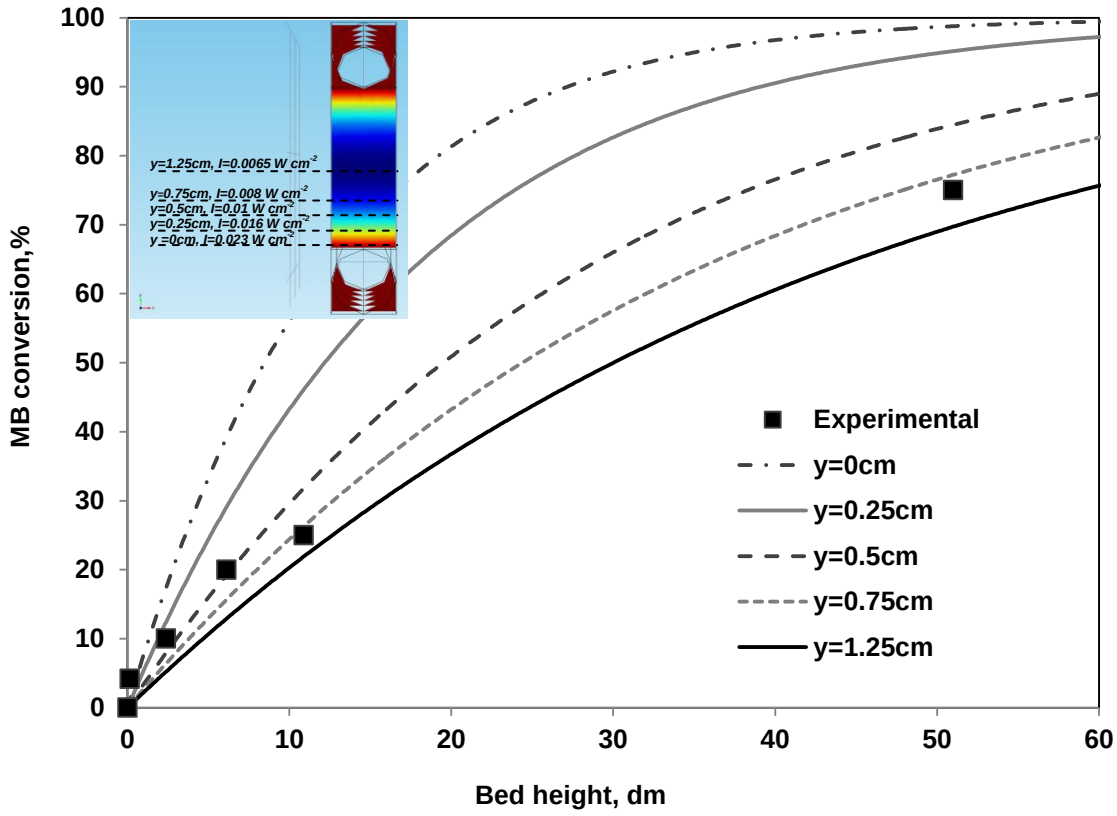

Figure 10 MB conversion as a function of the packed- bed height (z-direction) for different distances from the irradiated window (y-direction).